Retrieval of global hydrogen peroxide (H_2O_2) profiles using ENVISAT-MIPAS

E. Papandrea,[1,2] A. Dudhia,[1] R. G. Grainger,[1] X. Vancassel,[1] and M. P. Chipperfield[3]

Received 1 March 2005; revised 15 June 2005; accepted 17 June 2005; published 21 July 2005.

[1] We have used spectra from the Michelson Interferometer for Passive Atmospheric Sounding (MIPAS) to perform the first global retrievals of stratospheric H_2O_2. We demonstrate the feasibility of profile retrievals in the range 6–35 km and obtain zonal mean maps that average profiles computed from consecutive MIPAS orbits for the periods: December 2002, March, June and September 2003. The retrieved H_2O_2 values show an equatorial mid-stratospheric peak, enhanced values in the Antarctic springtime lower stratosphere, and diurnal/seasonal variability. Our retrieved H_2O_2 profiles are in qualitative agreement with expected photochemistry and with a previous balloon flight. **Citation:** Papandrea, E., A. Dudhia, R. G. Grainger, X. Vancassel, and M. P. Chipperfield (2005), Retrieval of global hydrogen peroxide (H_2O_2) profiles using ENVISAT-MIPAS, *Geophys. Res. Lett.*, *32*, L14809, doi:10.1029/2005GL022870.

1. Introduction

[2] Atmospheric hydrogen peroxide is formed primarily in the reaction [*Wayne*, 1991; *Dessler*, 2000]

$$HO_2 + HO_2 \rightarrow H_2O_2 + O_2, \quad (1)$$

although production can be suppressed in high NO_x regimes (in the troposphere) when the peroxy radical, HO_2, reacts with NO, i.e.

$$HO_2 + NO \rightarrow OH + NO_2. \quad (2)$$

Loss of H_2O_2 is principally through

$$H_2O_2 + OH \rightarrow H_2O + HO_2, \quad (3)$$

$$H_2O_2 + h\nu \rightarrow 2OH. \quad (4)$$

In the troposphere, the gas-phase reactions are augmented by the loss of dissolved H_2O_2 mainly through reaction with dissolved SO_2 and rainout [*Wayne*, 1991; *Seinfeld and Pandis*, 1998]. The photolytic loss mechanism should result in diurnal and seasonal variations in H_2O_2.

[3] Above 30–40 km, H_2O_2 is in photochemical equilibrium, while in the lower atmosphere the production and loss slows so that transport contributes to the global H_2O_2 distribution. Stratospheric H_2O_2 is important as it acts as a reservoir for odd hydrogen, HO_x (= HO_2 + OH + H), so reducing the amount of HO_x available to participate in catalytic cycles that deplete ozone [*Dessler*, 2000].

[4] Here, we describe the retrieval of H_2O_2 profiles using spectra obtained by the Michelson Interferometer for Passive Atmospheric Sounding (MIPAS). The results are examined for internal consistency and are compared against a chemical transport model and previous balloon measurements.

2. MIPAS Measurements of H_2O_2

2.1. MIPAS Instrument

[5] MIPAS was launched as part of Europe's environmental monitoring satellite, ENVISAT, aboard an Ariane-5 rocket on March 1, 2002. ENVISAT was injected into a polar orbit at an altitude of ~800 km and has an orbital period of about 100 minutes with a descending node mean local solar time (LST) of 10:00 am [*European Space Agency* (*ESA*), 2000a, 2000b]. MIPAS is an actively cooled atmospheric thermal emission limb sounder, working in the mid-infrared with a field-of-view that is approximately 3 × 30 km. MIPAS obtains high resolution spectra (0.035 cm^{-1} full width half maximum, unapodized) that cover the range 685–2410 cm^{-1} (14.6–4.15 μm). A complete limb scan sequence consists of 17 spectra with nominal tangent points at 68 km, 60 km, 52 km, 47 km, 42 km and then downward to 6 km in 3 km steps. The measurement time for a complete elevation scan is 70–80 s which corresponds to a horizontal sampling of 500–600 km between adjacent scans.

2.2. Preprocessing

[6] Often in limb profile retrievals the lower views are contaminated by clouds. In this study the cloud contaminated spectra have been removed from the analysis. A spectrum is considered cloudy if the ratio between the radiances of two small regions of the spectrum (788.20–796.25 cm^{-1} and 832.30–834.40 cm^{-1} [*Spang et al.*, 2004]) falls below the value of 1.8, as in the ESA MIPAS processor. Spectra have been apodized with the 'Norton-Beer strong' function [*Norton and Beer*, 1976].

2.3. Retrieval

[7] The ESA MIPAS processor code, called the Optimized Retrieval Model (ORM) [*Ridolfi et al.*, 2000] uses a least-square-fit approach and does not make use of *a priori* so it is unstable for minor species like H_2O_2. Therefore, we decided to perform the retrieval of H_2O_2

[1]Atmospheric, Oceanic and Planetary Physics, University of Oxford, Oxford, UK.
[2]On leave from Department of Physics and Inorganic Chemistry, University of Bologna, Bologna, Italy.
[3]Institute for Atmospheric Science, School of Earth and Environment, University of Leeds, Leeds, UK.

0094-8276/05/2005GL022870$05.00

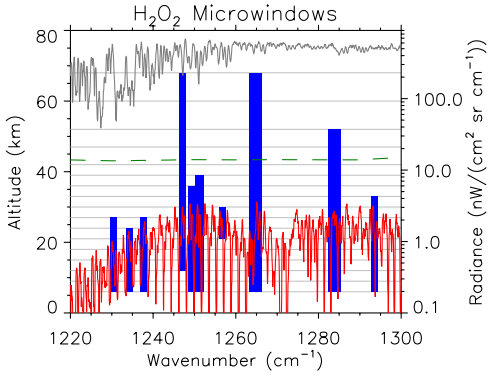

Figure 1. The region of the MIPAS spectrum containing the microwindows chosen for H_2O_2 retrieval (shaded blue regions), the instrument NESR (dashed line), H_2O_2 contribution (lower red line) and the total atmospheric radiance (upper line).

profiles from MIPAS with the Orbital Retrieval using Sequential Estimation (MORSE) algorithm. MORSE uses essentially the same forward model and retrieval algorithm as an earlier code, OPTIMO, the main features of which are summarised in the description of an intercomparison experiment of various MIPAS retrieval codes [*Von Clarmann et al.*, 2003]. The optimal estimation method offers the advantage of a more stable retrieval but the contribution of the *a priori* in the final results must be reduced as much as possible.

[8] In the retrieval the fitted quantities are ln(VMR) and atmospheric continuum. First pressure-temperature then water vapor were retrieved, all other interfering species were set to the climatological values. As initial *a priori* constraint we used a flat H_2O_2 *a priori* profile of 0.04 ppbv with an uncertainty of 1000% without any vertical correlation in order to avoid *a priori* information introducing vertical structure. The *a priori* value of 0.04 ppbv is in the middle of the retrieved values.

[9] In the MIPAS spectral range, hydrogen peroxide's main features are in the region 1190–1330 cm^{-1}, they are

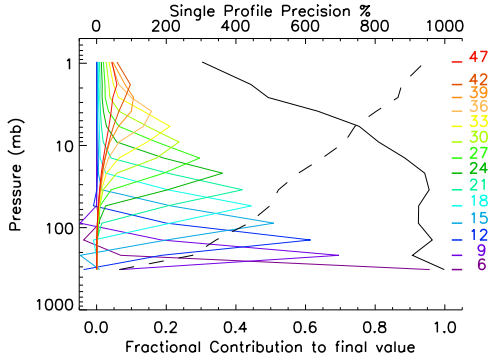

Figure 2. Representative averaging kernels (columns) for an equatorial night profile. The width of the kernels is a measure of retrieval resolution. The vector of area (black) and the estimated standard deviation (dashed) are also shown.

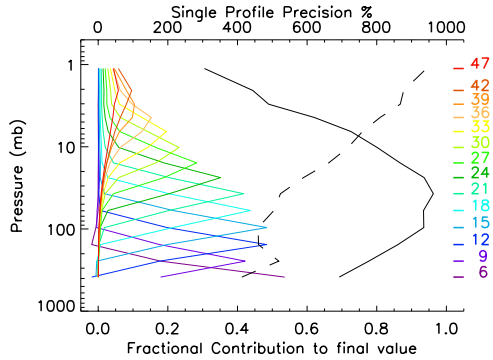

Figure 3. As Figure 2 but for a flat profile of 0.04 ppbv.

due to the ν_6 torsion - rotation band [*Perrin et al.*, 1990; *Rothman et al.*, 1998, 2003]. Rather than using all the available spectral data, it is more efficient to select microwindows, i.e. small regions of the spectrum [*Ridolfi et al.*, 2000; *Dudhia et al.*, 2002].

[10] Figure 1 shows the modelled H_2O_2 contribution to the limb radiance for the lower stratosphere. The H_2O_2 signal never exceeds the MIPAS Noise-Equivalent Spectral Radiance (NESR) for a single spectra measurement. The coverage of the ten selected microwindows is also shown, along with their tangent altitude range.

2.4. Post Processing

[11] As the main error source in the retrieval is the random error we can lower the errors by averaging profiles. Retrieval of several consecutive MIPAS orbits was performed in order to have a large number of profiles, which have been averaged in logarithmic domain. Results outside the mean $\pm 3\sigma$ have been removed (roughly about 0.5%).

2.5. Retrieval Diagnostic

[12] The microwindows error analysis shows that random error is the dominant error source in the retrieval and that the systematic error is smaller by an order of magnitude. An indicator of retrieval quality and information content is the averaging kernel **A** [*Rodgers*, 2000]. **A** is defined as:

$$\mathbf{A} = \mathbf{I} - \mathbf{S}_a^{-1}\mathbf{S}_x, \tag{5}$$

where **I** is the identity matrix, $\mathbf{S}_a$ and $\mathbf{S}_x$ are the variance-covariance of the *a priori* and of the retrieval.

[13] Figure 2 shows a representative averaging kernel from simulated spectra for a typical equatorial profile of H_2O_2. In the following results, we usually observe approximately five degrees of freedom (trace of the averaging kernel matrix), indicating that of the 14 levels retrieved there are 5 wholly independent points in the final retrieval. The most information-rich region is the troposphere and the lower stratosphere, due to the better signal-to-noise ratio. Below 3 mb the **A** value is more than 0.2 which means that the H_2O_2 retrieval is feasible in these regions while above 3 mb the sensitivity drops quickly. Figure 3 shows a representative averaging kernel from simulated spectra for a flat profile of 0.04 ppbv. Here the sensitivity decreases steadily with height.

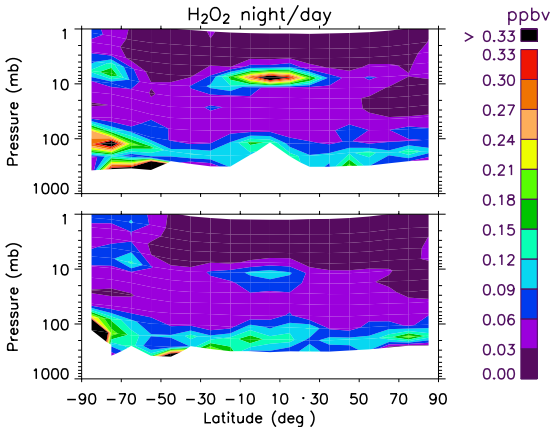

Figure 4. H_2O_2 latitude-height mean volume mixing ratio (ppbv) for the period 21–25 September 2003 for (top) nighttime and (bottom) daytime.

[14] The minimum retrievable value of 0.02 ppbv for H_2O_2 VMR has been obtained in a test performed on radiances simulated for an atmosphere without any H_2O_2.

3. Results

3.1. Zonal Mean Profiles

[15] The zonal mean profiles of night and day obtained from 5 consecutive days of September 2003 are shown in Figure 4. Roughly 100 profiles have been averaged so the uncertainty is expected to be reduced by a factor 10. At night we observe a peak of (0.40 ± 0.04) ppbv between

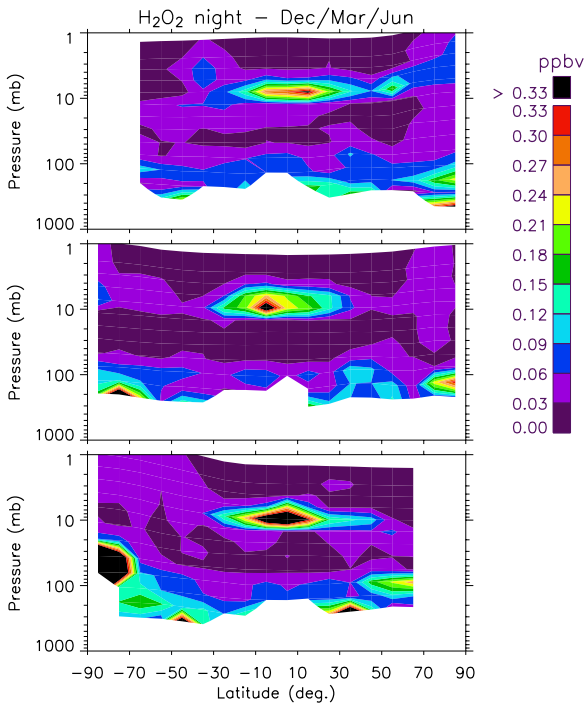

Figure 5. H_2O_2 zonal mean profiles for the periods (top) 20–25 December 2002, (middle) 20–25 March, and (bottom) 20–25 June 2003 during nighttime. In June/December there are no nighttime measurements polewards of 65°N/S due to polar day.

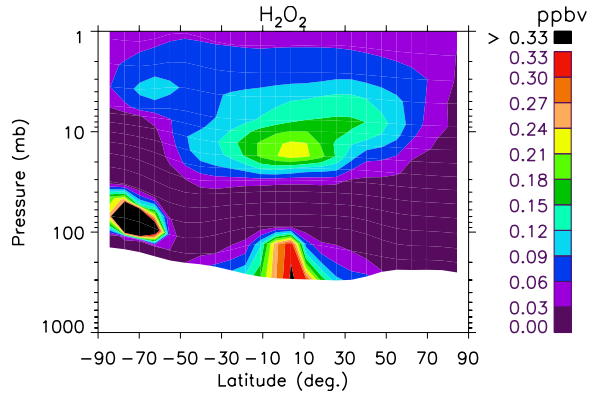

Figure 6. Zonal mean H_2O_2 (ppbv) from a simulation using the SLIMCAT 3D CTM for September 22, 2003.

10–7 mb (32–35 km) in equatorial regions: this partially disappears during the day, due to photolysis. Both daytime and nighttime there is also a peak between 200–30 mb (10–20 km) poleward of 70°S. There is no significant difference between day and night in other regions.

[16] We investigated seasonal variability, analyzing zonal means for different periods of a whole year: the December solstice of 2002, the March equinox and the June solstice of 2003 have been analyzed. These zonal mean profiles are shown in Figure 5. In all these panels there is a peak of H_2O_2 in equatorial regions between 6–7 mb and 10–15 mb. In December this stratospheric peak is less evident; in June there is another peak around the south pole. These equatorial stratospheric peaks appear consistent with the H_2O_2 physical chemistry as HO_2, the precursor of H_2O_2, is formed through the reaction:

$$OH + O_3 \rightarrow HO_2 + O_2. \quad (6)$$

3.2. Comparison With SLIMCAT 3D Model and FIRS-2–BMLS

[17] As there are no other global observations of H_2O_2 we have compared our data with output from the SLIMCAT 3-D chemical transport model (CTM) [*Chipperfield*, 1999] in order to check its consistency with current photochemical theories. The SLIMCAT CTM has been widely used in stratospheric studies and contains a detailed stratospheric chemistry scheme. We use output from a multiannual SLIMCAT simulation with a resolution of 7.5° × 7.5° with 18 levels from 8 to 60 km. Photochemical data was taken from *Sander et al.* [2003].

[18] Figure 6 shows the zonal mean H_2O_2 from SLIMCAT for September 22, 2003. Overall, there is good agreement between the model and observations. The model reproduces the stratospheric equatorial peak although the zonal mean smears out the larger observed nighttime peak. Interestingly, the model also reproduces the high H_2O_2 concentrations observed in the Antarctic lower stratosphere. These are due to the perturbed ClO_x/HO_x chemistry during the ozone hole period.

[19] The nighttime profile at 35°N is also in very good agreement with the in situ measurements made from a balloon flight with the Smithsonian Astrophysical Observa-

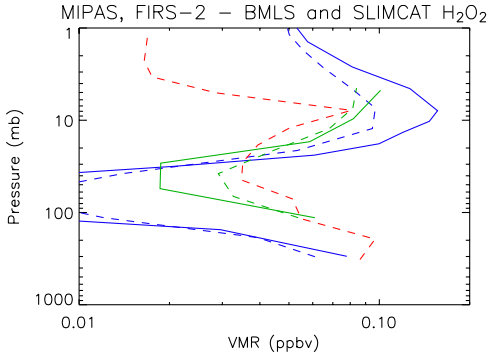

Figure 7. H_2O_2 profiles for about 35°N from SLIMCAT for September 22, 2003 (solid blue) and from night balloon measurements for September 26, 1989 (solid green). Assuming these are the 'real' atmosphere what we would retrieve is represented by the respective dashed lines. The dashed red line shows the MIPAS retrieved night mean profile for the period 21–25 September 2003.

tory Far-Infrared Spectrometer (FIRS-2) and the Jet Propulsion Laboratory Balloon Microwave Limb Sounder (BMLS) in September 26, 1989 [*Chance et al.*, 1996], as shown in Figure 7. The dashed profiles are obtained multiplying the FIRS-2–BMLS and SLIMCAT profiles with the averaging kernel.

4. Conclusions

[20] We have demonstrated the feasibility of profile retrievals in the range 6–35 km from ENVISAT-MIPAS based on single scans, with about 5 degrees of freedom for each profile. Our data show a peak in H_2O_2 in the equatorial stratosphere and large values in the Antarctic ozone hole region. We also find some night - day variations in the H_2O_2 concentrations. Our retrieved profiles are in reasonable agreement with expected photochemical behaviour and with a previous balloon profile.

[21] Future work will make use of the wealth of available MIPAS data for the study of other minor species which are involved in the H_2O_2 equilibrium (i.e. HO_2) for a better understanding of the H_2O_2 physical chemistry and the study of annual variations of H_2O_2.

[22] **Acknowledgments.** E. Papandrea is grateful to M. Carlotti (University of Bologna) for his support and advice in preparing this paper and the Marco Polo fellowship for the funds. The authors acknowledge funds, from the NERC EO Enabling Fund (NER/T/S/2003/00135) for MORSE.

References

Chance, K., et al. (1996), Simultaneous measurements of stratospheric HO_x, NO_x, and Cl_x: Comparison with a photochemical model, *J. Geophys. Res.*, *101*, 9031–9043.

Chipperfield, M. P. (1999), Multiannual simulation with a three-dimensional chemical transport model, *J. Geophys. Res.*, *104*, 1781–1805.

Dessler, A. (2000), *The Chemistry and Physics of Stratospheric Ozone*, Elsevier, New York.

Dudhia, A., V. Jay, and C. Rodgers (2002), Microwindows selection for high spectral resolution sounders, *Appl. Opt.*, *41*, 3665–3673.

European Space Agency (ESA) (2000a), Envisat-1: Mission and system summary, *Eur. Space Agency Sci. Tech. Rep.*, *ESA/SP-1229*, 85 pp.

European Space Agency (ESA) (2000b), Envisat MIPAS—An instrument for atmospheric chemistry and climate research, *ESA Bull.*, *101*, 14 pp.

Norton, R. H., and R. Beer (1976), New apodizing functions for Fourier spectrometry, *J. Opt. Soc. Am.*, *66*, 259–264. (Correction, *J. Opt. Soc. Am.*, *67*, 419, 1977.)

Perrin, A., et al. (1990), New analysis of the v6 band for hydrogen peroxide: The (n, τ) = (0,1), (1,1), (2,1), (0,3), and (1,3) torsional subbands, *J. Mol. Spectrosc.*, *142*, 129–147.

Ridolfi, M., et al. (2000), Optimized forward model and retrieval scheme for MIPAS near-real-time data processing, *Appl. Opt.*, *39*, 1323–1340.

Rodgers, C. D. (2000), *Inverse Methods for Atmospheric Sounding: Theory and Practice*, World Sci., Hackensack, N. J.

Rothman, L., et al. (1998), The HITRAN molecular spectroscopic database and HAWKS (HITRAN atmospheric workstation): 1996 edition, *J. Quant. Spectrosc. Radiat. Transfer*, *60*, 665–710.

Rothman, L., et al. (2003), The HITRAN molecular spectroscopic database: Edition of 2000 including updates through 2001, *J. Quant. Spectrosc. Radiat. Transfer*, *82*, 5–44.

Sander, S. P., et al. (2003), Chemical kinetics and photochemical data for use in stratospheric modeling, Update to Evaluation no. 14, *JPL Publ., 02-25*, 334 pp.

Seinfeld, J. H., and S. N. Pandis (1998), *Atmospheric Chemistry and Physics*, John Wiley, Hoboken, N. J.

Spang, R., J. Remedios, and M. Barkley (2004), Colour indices for the detection and differentiation of cloud types in infra-red limb emission spectra, *Adv. Space Res.*, *33*, 1041–1047.

Von Clarmann, T., et al. (2003), A blind test retrieval experiment for infrared limb emission spectrometry, *J. Geophys. Res.*, *108*(D23), 4746, doi:10.1029/2003JD003835.

Wayne, R. P. (1991), *Chemistry of Atmospheres*, Clarendon, Oxford, UK.

M. P. Chipperfield, Institute for Atmospheric Science, School of Earth and Environment, University of Leeds, Leeds LS2 9JT, UK.

A. Dudhia, R. G. Grainger, and X. Vancassel, Atmospheric, Oceanic and Planetary Physics, Clarendon Laboratory, University of Oxford, Parks Road, Oxford OX1 3PU, UK.

E. Papandrea, Department of Physics and Inorganic Chemistry, University of Bologna, Via Risorgimento 4, I-40136 Bologna, Italy. (enzo@safire.fci.unibo.it)